240 Transaction of the Korean Society of Mechanical Engineers, Vol. 9, No. 2, pp. 240~249, 1985.

<Original>

An Indirect Experimental Method for the Determination of Mechanical Properties of Ion-nitrided Layer and Residual Stress Distribution

Byung Man Kwak* and Young-Jun Gil**

(Received December, 8 1984)

이온질화층의 기계적 성질과 잔류응력 분포를 위한 간접 실험법

곽 병 만·길 영 준

Key Words: Ion-nitrided layer, Thermal expansion coefficient, Elastic modulus, Axial extension, Residual stress

초 록

여러가지 조건하에서 한쪽면만 이온질화 처리된 SCM 4의 평판을 모델로 하여 질화층의 기계적 성질과 잔류응력을 연구하였다. 질화층에서의 재료의 성질은 질소함량분포에 비례하여 변할 것이라는 가정하에 외팔보의 굽힘과 온도—곡률의 관계를 구하는 이론적 모델을 정립하고 이에 따른 간접적 실험방법을 제시하였다.

질화층 표면에서의 선팽창 계수는 질화되지 않은 코어의 값에 비해 2내지 12% 증가를 보였고 탄성계수는 50내지 700% 증가를 보였다. 질화로 인한 축방향 팽창은 변형도로 약 0.002를 얻었다. 상온에서의 코어의 최대 인장 잔류응력은 2내지 25 kg/mm² 이며, 질화층표면에서 일어나는 최대압축잔류응력은 질화조건에 따라 50내지 300 kg/mm²을 얻었다.

1. Introduction

Nitriding[1,2,3] is widely used as a surface treatment of machine parts operating under cyclic stresses and severe wear conditions. Much literature[4,5,6] is available regarding the effects of ion-nitriding parameters such as time, temperature, pressure, gas composition and voltage upon gross mechanical properties such as hardness, wear and fatigue. Few papers, however, deal with the changes in local mechanical properties due to ionnitriding and their correlation to gross properties. Jones and Martin[7] obtain-

*Member, Korea Advanced Institute of Science and Technology
**Graduate Student

ed a residual stress distribution in nitrided En 41 B steel as a function of case depth by the Sachs boring technique. The elastic properties in the nitrided specimen were obviously assumed uniform which is very doubtful.

In this study, the change of elastic modulus and thermal expansion coefficient of the nitrided layer is assumed occurring due to ion-nitriding and an indirect experimental method based on a theoretical model is proposed to find these local property change and the resulting residual stress distributions in flat specimens without destruction of the material.

The basic procedure of the method may be summarized as follows. Theoretical formulas for the response of a specimen under force and temperature loading are first derived. The calculated responses are then used to match the measured responses under the same loadings by finding unknown parameters contained in the formulas. Once the parameters, which are related to the local property change, are obtained, the residual stress in the specimen can be easily calculated.

2. Analyical Model

2.1. Problem Definition and Assumptions

The main objective is to find the distribution of residual stress in an ion-nitrided beam with length L, thickness $2h$, and width b. If the beam is split into two parts along the centroidal line, each part will be curved.

The same result is obtained when only one surface of a beam with thickness h is nitrided by masking opposite surface. The residual stresses in the curved state and in the straightened state will be considered. A previous study by the author[8] was based on the assumption that the nitrided beam is composed of two homogeneous layers; nitrided layer and non-nitrided core layer. In this study, this idea will be further elaborated.

Following(8), it is assumed that the mechanical properties of the core material remain unchanged after nitriding. The compound layer which is about 10 μm is negligible for the mechanical analysis, comparing with the diffusion layer which is about 400 μm. The other assumption introduced here is that the changes in material properties are proportional to the amount of nitrogen concentration. It is reported[9,10] that there exists an almost linear relationship between nitrogen content and measured hardness values. In this paper for the analytical model, it is assumed that the changes in the elastic modulus, thermal expansion coefficient and voluminal extension are primarily dependent only on the nitrogen concentration and proportional to it. The nitrogen concentration is taken from the solution of one dimensional diffusion problem for the present flat specimen:

$$\frac{c}{c_s}=\mathrm{erfc}\frac{\eta}{2\sqrt{Dt}} \tag{1}$$

where η is the depth from the surface, c_s the surface concentration, D the diffusion constant and t the nitriding time. The symbol erfc denotes the complementary error function.

The forms for Young's modulus $E(\eta)$, thermal expansion coefficient $\alpha(\eta)$, and the axial extension $\varepsilon^*(\eta)$ are then given as follows:

$$E(\eta)-E_c=E_p\cdot\mathrm{erfc}\frac{\eta}{2\sqrt{Dt}} \tag{2}$$

$$\alpha(\eta)-\alpha_c=\alpha_p\cdot\mathrm{erfc}\frac{\eta}{2\sqrt{Dt}} \tag{3}$$

$$\varepsilon^*(\eta)=\varepsilon_s\cdot\mathrm{erfc}\frac{\eta}{2\sqrt{Dt}} \tag{4}$$

where, E_c denotes Young's modulus of non-nitrided core; α_c thermal expansion coefficient of non-nitrided core; E_p change of Young's modulus at the nitrided surface; α_p change of thermal expansion coefficient at the nitrided surface; and ε_s normal extension in terms of

strain due to the voluminal increase by nitriding. The diffusion coefficient D is taken from the following equation[11],

$$\ln D=-4.485-0.9979\,\xi+0.0014\,\xi^2 \quad (5)$$

where $\xi=(10^4/T)$ and T denotes the absolute temperature in Kelvin, and D is in cm^2/sec.

Residual stresses arise basically from two sources. The first source is the thermal residual stress due to the difference in thermal expansion coefficient, and the other is due to uneven axial extension. In order to find these stresses, it is necessary to know the mechanical properties(Young's modulus and thermal expansion coefficient), the amount of axial extension and the boundary condition.

2.2. Thermal Stress, σ_{th}

Following Boley and Weiner[12], the strain and stress in a beam, when they are independent of the axial location, are expressed as,

$$\varepsilon_{xx}=\frac{\partial u}{\partial x}=a_0+a_1 y \quad (6)$$

$$\sigma_{th}=\sigma_{xx}=E(y)\cdot[\varepsilon_{xx}-\alpha(y)\cdot\Delta T]$$
$$=E(y)\cdot[a_0+a_1 y-\alpha(y)\cdot\Delta T] \quad (7)$$

where $E(y)$ and $\alpha(y)$ are functions of y as obtained by substituting $\eta=y+\frac{h}{2}$ in Eqs. (2) and (3). The coordinate y is measured normal to the beam from the centroidal plane as in Fig. 1. ΔT is the temperature difference between some temperature T and a reference temperature. In this approximate analysis, the other stress and strain components are neglected and the beam is assumed free of external loads.

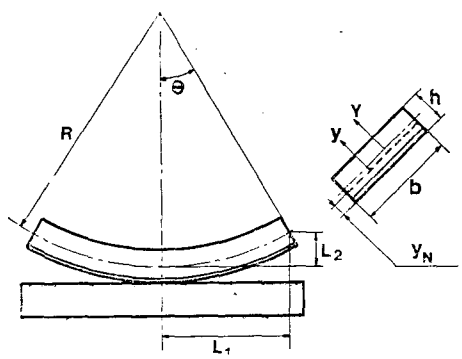

Fig. 1 Coordinate system for the cross-section and notation for the curvature measurement

The constants a_0 and a_1 are determined so as to satisfy equilibrium, that is

$$\int\sigma_{xx}\cdot dA=0=\int\sigma_{xx}\cdot y\cdot dA \quad (8)$$

where the integration is extended over the entire cross-sectional area. Therefore,

$$a_0=\frac{1}{\mathrm{Det}}\begin{vmatrix}\int E(y)\cdot\alpha(y)\cdot\Delta T\cdot dA & \int E(y)\cdot y\cdot dA\\ \int E(y)\cdot\alpha(y)\cdot y\cdot\Delta T\cdot dA & \int E(y)\cdot y^2\cdot dA\end{vmatrix} \quad (9)$$

$$a_1=\frac{1}{\mathrm{Det}}\begin{vmatrix}\int E(y)\cdot dA & \int E(y)\cdot\alpha(y)\cdot\Delta T\cdot dA\\ \int E(y)\cdot y\cdot dA & \int E(y)\cdot\alpha(y)\cdot y\cdot\Delta T\cdot dA\end{vmatrix} \quad (10)$$

where

$$\mathrm{Det}=\begin{vmatrix}\int E(y)\cdot dA & \int E(y)\cdot y\cdot dA\\ \int E(y)\cdot y\cdot dA & \int E(y)\cdot y^2\cdot dA\end{vmatrix}$$

2.3. Residual Stress due to Extension, σ_e

The normal extension by interstitial diffusion of nitrogen atoms, generated after nitriding is considered. Consider a beam of thickness h and width b such that both b and h are small compared to the length L. Let the residual stress due to the normal extension be denoted by $\sigma_e(y)$. Because of the thinness of the beam, the plane stress assumption is made,

$$\sigma_{yy}=\sigma_{xy}=\sigma_{yz}=0. \quad (11)$$

The solution of the resulting two dimensional problem can be obtained by making the semi-inverse assumption such that

$$\sigma_{zz}=\sigma_{xz}=0,\quad \sigma_{xx}=\sigma_{xx}(y)=\sigma_e \quad (12)$$

The equations of equilibrium are then satisfied identically and strain components are obtained

$$\varepsilon_{yy}=\varepsilon_{zz}=\varepsilon_{xy}=\varepsilon_{yz}=\varepsilon_{xz}=0 \tag{13}$$

$$\varepsilon_{xx}=\frac{\sigma_e}{E(y)}+\varepsilon^*(y) \tag{14}$$

where $\varepsilon^*(y)$ is given by Eq. (4). Therefore, the compatibility equation in terms of strains reduces in this case to

$$\frac{d^2}{dy^2}\left[\frac{\sigma_e}{E(y)}+\varepsilon^*(y)\right]=0 \tag{15}$$

Hence, σ_e is obtained as

$$\sigma_e(y)=E(y)[-\varepsilon^*(y)+c_1+c_2y]. \tag{16}$$

The constants c_1 and c_2 are determined by the equilibrium conditions,

$$\int\sigma_e dy=0, \tag{17}$$

$$\int\sigma_e y dy=0 \tag{18}$$

or

$c_1=\phi_1\cdot\varepsilon_s$ and $c_2=\phi_2\cdot\varepsilon_x$

where ϕ_1 and ϕ_2 are coefficients, and the integration is over the cross-sectional area. The constant c_1 represents the average axial strain due to the voluminal increase by nitriding.

2.4. Straightening Stress, σ_{st}

The residual stresses in the straightened nitrided beam is obtained by superposing the stress which is necessary to straighten the curved nitrided beam.

For a pure bending of a rectangular beam, the bending stress σ_b, is

$$\sigma_b=-\frac{E(Y)}{R}\cdot Y \tag{19}$$

where Y is measured from the neutral surface, as seen in Fig. 1. And hence $Y=y+\frac{h}{2}-y_N$. R denotes the radius of curvature before straightening. This expression must satisfy the requirements that the resultant be zero and the moment of the internal forces about the neutral axis be equal to the straightening moment M_z. That is,

$$\int\sigma_b\cdot dA=0, \tag{20}$$

$$\int\sigma_b\cdot Y\cdot dA=-M_z \tag{21}$$

Equation (20) may be written as

$$\int_{-y_N}^{h-y_N}E(Y)\cdot Y\cdot dY=0 \tag{22}$$

Therefore, this expression gives y_N as a function of $E(Y)$. Also, Eq.(21) can be rearranged as,

$$M_R=\frac{RM_z}{b}=\int_{-y_N}^{h-y_N}E(Y)\cdot Y^2\cdot dy, \tag{23}$$

where M_R denotes the straightening moment times the radius of curvature divided by the width. The integral denotes the effective bending stiffness.

Equations (22) and (23) will be used to find the parameter E_p in the next section. Therefore, if $E(Y)$ is given, the residual stress necessary to straighten the beam can be written as

$$\sigma_{st}=-\sigma_b=\frac{E(Y)}{R}\cdot Y \tag{24}$$

The total residual stress is then obtained as

$$\sigma=\sigma_{th}+\sigma_e+\sigma_{st} \tag{25}$$

For a curved nitrided beam, σ_{st} is zero.

2.5. Method of Parameter Determination

The residual stress can be obtained once the unknowns, E_p, α_p, ΔT, M_R, ε_s, c_1 and c_2 are determined. Four conditions, (17), (18), (22) and (23) are available and the other necessary information for the knowns comes from the behavior of the specimen under actual loading of direct force and temperature change.

The normalized moment M_R can be found from a deflection test of a cantilever set-up. For a beam with varying elastic modulus, the deflection $v(x)$ for a load W at a distance a ($\leq x$) from the fixed end is,

$$v(x)=\frac{Wa^2}{6\cdot M_R}(3x-a). \tag{26}$$

From the measurements of v for different loading, M_R can be estimated. From Eqs. (2), (22) and (23), a quadratic equation in E_p is obtai-

ned. Physically, E_p must be positive.

The unknowns ΔT(or reference temperature T_0), ε_s and α_p can be found by measuring the curvature of nitrided beam under various temperature changes. The curvature $1/R$ is composed of two parts for the specimen. One is due to thermal stress σ_{th} and the other is due to σ_e. That is,

$$\frac{1}{R}=\frac{1}{R_{th}}+\frac{1}{R_e} \tag{27}$$

where $\frac{1}{R_e}$ remains unchanged and $\frac{1}{R_{th}}$ varies with temperature. The reference temperature T_0, here, is defined as the temperature for which $\frac{1}{R_{th}}$ is zero.

Two cross sections of the beam, initially lying in the planes $x=x_1$, and $x=x_1+dx_1$ will be inclined to each other as temperature changes. Their final positions may be described by the following equations,

$$x=x_1+u(x_1, y, z) \tag{28}$$

and

$$\begin{aligned} x&=x_1+dx_1+u(x_1, y, z)+\frac{\partial u}{\partial x_1}dx_1 \\ &=x_1+u(x_1, y, z)+(1+a_0+a_1y)dx_1 \end{aligned} \tag{29}$$

respectively, where $\frac{\partial u}{\partial x_1}=\varepsilon_{xx}$, is given by Eq. (6). The angle between these two planes on the xy plane is related to the radius of curvature R_{th} in (27). Based on the assumption of small deformations,

$$-\frac{1}{R_{th}}=\frac{d\phi}{dx_1} \tag{30}$$

From the geometry, using Eqs. (29) and (30), $d\phi$ is expressed as

$$\begin{aligned} d\phi=&\frac{1}{y}[\{x_1+u(x_1, y, z_1)+(1+a_0+a_1y)dx_1 \\ &-x_1-u(x_1, y, z_1)\}-\{x_1+u(x_1, 0, z_1) \\ &+(1+a_0+0.\,a_1)dx_1-x_1-u(x_1, 0, z_1)\}] \\ =&a_1dx_1 \end{aligned}$$

Therefore, from Eq. (30)

$$\frac{d\phi}{dx_1}=-\frac{1}{R_{th}}=a_1 \tag{31}$$

Since a_1 is a linear function of ΔT and $1/R_e$ is a constant, from Eqs. (10), (27) and (31), the following temperature-curvature relation is obtained,

$$\frac{1}{R}=AT+B \tag{32}$$

where A and B are constants. This shows that curvature found by experiment must be fitted into a linear function of temperature. Since the coefficient of ΔT in Eq. (10) is equal to $-A$, once A is estimated from experiments, α_p can be obtained using Eq. (10).

In order to find T_0 and ε_s, consider the relationship between $\frac{1}{R}$ and the total strain which means thermal strain plus strain due to extension. At room temperature, $T_r(=15°C)$, it can be expressed as

$$-\frac{Y}{R_r}=(c_1+c_2y)+(a_0+a_1y) \tag{33}$$

where, $Y=y+\frac{h}{2}-y_N$

$$\frac{1}{R_r}=AT_r+B$$

$$c_1=\phi_1\varepsilon_s$$

$$c_2=\phi_2\varepsilon_s$$

$$a_1=-A(T_r-T_0)$$

$$a_0=\phi_3(T_r-T_0)$$

and ϕ_3 is a constant obtained from Eq. (9). Since Eq. (33) is an identity, that should be satisfied for all y, one has

$$-\frac{1}{R_r}=\phi_2\varepsilon_s-A(T_r-T_0) \tag{34}$$

and

$$-\frac{1}{R_r}\left(\frac{h}{2}-y_N\right)=\phi_1\varepsilon_s+\phi_3(T_r-T_0) \tag{35}$$

by comparing the coefficients. Solving for ε_s and T_0,

$$\varepsilon_s=\frac{A\left(y_N-\frac{h}{2}\right)-\phi_3}{A\phi_1+\phi_2\phi_3}\frac{1}{R_r} \tag{36}$$

and

$$T_0=-\frac{\phi_2\varepsilon_s+B}{A} \tag{37}$$

3. Experiments

Fifteen specimens were prepared from round bars of SCM 4 by milling, surface grinding and then annealing. The chemical composition is shown in Table 1. The dimension of specimens are $L=100\pm0.1$ mm, $b=9\pm0.5$ mm and $h=2\pm0.05$ mm. These specimens were ion-nitrided at three different temperatures, 450°C, 500°C and 550°C with 1, 2, 3, 5 and 7 hours of treating time for each temperature. The ion-nitriding equipment used has 30 kW capacity, with a vacuum chamber of 70 cm diameter and 120cm height. It was developed at the author's laboratory. The ambient gas used is 80% N_2 and 20% H_2 mixed at a pressure of 5 Torr. The treated specimens are air-cooled in the chamber.

Table 1 Chemical composition of specimen materials

Component	Si	Mn	P	Cr	Mo	C	Fe
% by Wt.	0.25	0.72	0.015	0.097	0.014	0.44	Balance

Using a dial guage with a resolution of 0.01 mm, deflections of the nitrided specimens were measured five times and averaged. A load of 100.54 g was used. The loading point and deflection measuring point were kept at 58 and 88 mm, respectively.

For the temperature response measurement, a box type furnace was utilized. Pictures of the nitrided specimen tied to a reference straight beam of the same material were taken at various temperatures from the room temperature up to the nitriding temperature by a step of 50°C. Temperature of the specimen was measured indirectly by measuring that of the reference specimen by Chromel-Alumel type thermocouple. The half span L_1 and height L_2 of the curved specimen as shown in Fig. 1 were measured on the film with a travelling microscope. The relation between the curvature $1/R$ and the measured distances L_1 and L_2 is found, from the geometry as,

$$\frac{1}{R}=\frac{2L_2}{L_1^2+L_2^2} \tag{38}$$

Microhardnesses of the nitrided specimens were measured in order to obtain the case depth. The case depth was defined as the distance from the nitrided surface to the point from which almost constant hardness is obtained. A microhardness tester(Wilson Instrument Division, USA) with 100 g load was used. Vickers hardness was obtained from the nitrided surface at 0.001−0.002 inch intervals.

4. Results

4.1. Elastic Modulus

Table 2 summarizes the mechanical properties as obtained from the experiments using the analytical model as explained earlier. Values of Young's modulus at the nitrided surface, E_p+E_c, are given in the third column. The Young's modulus at the nitrided surface is increased by 50 to 700%. The value increases as the nitriding time and temperature increase. The value of non-nitrided specimen, $E_c=2.00\times10^4$ kg/mm^2 has been determined from deflection tests of non-nitrided specimen.

4.2. Thermal Expansion Coefficient

The value of thermal expansion coefficient at the nitrided surface, $\alpha_p+\alpha_c$, are obtained as shown in the fourth column. Thermal expansion coefficient at the nitrided surface is increased by 2 to 12% over the value of non-nitrided specimen, $\alpha_c=12.6\times10^{-6}$/°C as measured separately in the Institute. This change is small compared with the change in Young's modulus and it shows negligible, trend with respect to

Table 2 Mechanical properties and residual stresses

Nitriding conditions		Mechanical properties at the surface			Residual stress(kg/mm²) at the surface for flat beam				Peak tensile residual stress (kg/mm²)	Depth to $\sigma_{res}=0$ (mm)	case Depth (mm)
Temperature	Time, hrs	E_p+E_c (10^4kg/mm²)	$\alpha_p+\alpha_c$ (10^{-6}/°C)	ε_s (10^{-3})	σ_{res}	σ_θ	$\sigma_{\Delta t}$	σ_e			
450°C	1	2.11	13.8	2.37	−47.6	0.17	−5.90	−41.8	2.01	0.21	0.10
	2	7.60	14.2	1.64	−106.	1.31	−29.5	−77.7	4.31	0.23	0.18
	3	9.10	14.2	1.40	−103.	1.52	−33.8	−70.3	4.88	0.25	0.30
	5	11.5	13.2	1.70	−146.	1.08	−56.5	−90.9	8.20	0.27	0.36
	7	16.1	13.0	1.93	−210.	1.18	−88.6	−123.	12.1	0.27	0.41
500°C	1	2.64	13.8	2.03	−49.2	0.27	−10.1	−39.4	3.01	0.29	0.13
	2	7.59	13.0	1.48	−90.4	0.307	−32.7	−58.0	5.62	0.30	0.28
	3	7.09	13.3	2.15	−118.	0.816	−47.6	−71.6	9.14	0.35	0.36
	5	12.4	13.0	2.31	−190.	0.923	−91.0	−99.6	15.1	0.35	0.41
	7	13.5	12.8	2.63	−221.	0.747	−116.	−106.	19.5	0.38	0.48
550°C	1	4.27	13.3	2.80	−102	0.555	−33.6	−68.6	7.94	0.34	0.30
	2	8.99	13.4	2.22	−142	1.39	−64.5	−78.6	12.0	0.37	0.30
	3	12.1	13.5	2.11	−161.	1.90	−82.2	−80.6	14.5	0.38	0.45
	5	13.5	13.4	3.92	−299.	3.18	−178.	−124.	31.8	0.42	0.48
	7	15.2	13.6	3.90	−311.	3.76	−203.	−113.	34.5	0.46	0.52

the nitriding time.

4.3. Normal Extension

The normal strain ε_s due to the voluminal increase at the nitrided surface is obtained as shown in the fifth column. It shows a tendency of slight increase with increasing nitriding temperature and time. No significant variation, however, is observed in the test range. Its order is about 0.002 in terms of strain.

4.4. Distribution of Residual Stresses

The peak residual stresses in the straightened nitrided beams are compressive and occur on the nitrided surface. They are shown in Table 2 along with individual contributions, as obtained for various nitriding conditions. The results show a tendency of increase of residual stress with nitriding time and temperature as expected. The peak value increases almost proportionally with the nitriding time in the first few hours and then levels off.

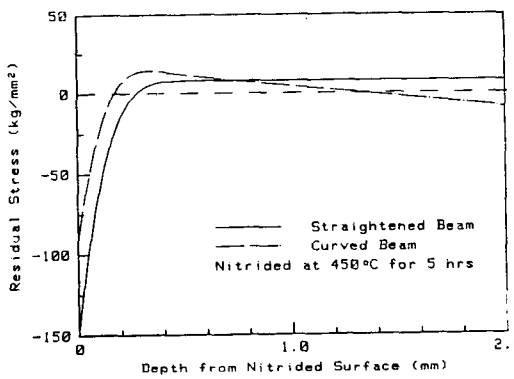

Fig. 2 Residual stress distributions at room temperature for the straightened and curved specimen treated for 5 hours at 450°C.

A representative pattern of residual stress distribution along the depth for a straightened specimen treated at 450°C for 5 hours is shown in Fig. 2. For this case, the values of various parameters obtained are: $b=8.98$ mm, $h=1.99$ mm, $D=0.150\times10^{-5}$ mm²/sec, $A=0.247\times10^{-6}$ /°C/mm, $B=0.665\times10^{-3}$/mm, $y_N=0.73$ mm,

$R_r=1496$ mm, $T_r=47.6°C$, $a_0=-0.414\times10^{-3}$, $a_1=0.807\times10^{-5}$, $c_1=0.239\times10^{-3}$, $c_2=-0.677\times10^{-3}$, $E_p=95200$ kgf/mm², $\alpha_p=0.622\times10^{-6}$/°C and $\varepsilon_s=0.00170$.

The very high compressive stress on the nitrided surface diminishes rapidly in about 0.5 mm depth and a residual tensile stress peak appears. The peak compressive residual stress shows a magnitude of about 50 to 300 kg/mm² depending on the nitriding conditions tested, while the peak tensile residual stress is about 2 to 25 kg/mm², as shown in Table 2. The dashed curve in the same figure denotes the residual stress distribution for the same specimen, but in the curved configuration of the same specimen at room temperature. In this shape, the non-nitrided opposite surface carries compressive residual stress. The difference between these two curves represents the residual stress due to the straightening moment. It is found that the thermally induced residual stress σ_{th} due to the change of thermal expansion coefficient is relatively small(less than 1%) compared with the other two contributions, σ_e and σ_{st}.

The case depth obtained by the measurement of microhardness does not coincide with the depth to the point of zero residual stress. The case depth varies more rapidly with the nitriding time than the nitriding temperature. However, the depth to zero residual stress varies more rapidly with the temperature than the time.

5. Discussions

With the hypothesis that the changes in mechanical properties such as Young's modulus, thermal expansion coefficient and the lattice parameter in the diffusion layer are proportional to the nitrogen concentration, an indirect experimental method was developed. This assumption, although not proven, was introduced based on the intuitive observation that the hardness is very similarly distributed as the nitrogen concentration and that the yield stress and Young's modulus show a trend of linear proportion with the hardness.

The maximums of the mechanical properties and residual stresses, occurring at the nitrided surface are considered somewhat overestimated. The results in(7) by the Sachs boring technique show similar pattern. From the present predictions, the mechanical property change can be very large and this suggests that the application of the Sachs boring method is not proper when this change is not included in the formula.

One reason for the overestimation of the peak residual stress is because the compound layer is neglected in the analytical model although it is about one 40th of the nitrided layer. The nitrogen concentration in this layer is rather uniform as directly measured[13] and hence the sharp increase at the surface will be lowered although the effect is found small. The distribution of the nitrogen concentration in the diffusion layer and core seems closely following the solution of the one dimensional diffusion equation[13]. However since the diffusion coefficient for the nitrogen in the SCM 4 was not available, the value for pure iron, Eq.(5) was used in the calculation. Diffusion coefficient is also a strong function of concentration[14]. These can be a source of error in the presert predictions. Moreover, it is found that the effect of diffusion coefficient on the final residual stress is relatively large. Therefore a proper diffusion coefficient needs to be obtained for a better prediction of properties.

Another reason for the overestimation may come from the sputtering effect. The sputtering is reported to reduce the increase of lattice parameters[5] and hence will reduce the peak re-

sidual stress at the nitrided surface.

Consideration of the local changes in the mechanical proporties, not as global properties, is very different from other studies in the literature. This suggests a new approach for the study of global mechanical properties of a given specimen. The information about the distribution of Young's modulus, for example, can be essential to the explanation of fatigue and wear characteristics, because it allows more realistic estimation of local stresses. The normal extension is also essential in the prediction of dimensional change of nitrided parts. These and other global mechanical properties are under study in relation to the results of the present study.

6. Conclusions

An indirect experimental method combined with analytical relations was developed to determine the distribution of elastic modulus and thermal expansion coefficient, from which residual stresses were obtained. The method is unique in that it considers the detailed change of mechanical properties along the depth and finds individual contributions to the total residual stresses.

Although direct verification is lacking, the results obtained seem very reasonable and supply the basic data necessary to estimate changes of global mechanical properties. The linearity assumptions introduced regarding various distributions, however, remain to be tested and the diffusion coefficient and measurement technique in high temperature need be refined.

Acknowledgement

This study was partially supported by the Korea Science and Engineering Foundation.

References

(1) Edenhofer, B., "Physical and Metallurgical Aspects of Ionitriding," Part 1, Heat Treatment of Metals, 1, pp. 23~28; Part 2, 1974. 2, pp. 59~67, 1974.

(2) Lakhtin, Yu. M., Krymskii, Yu. N., and Semenov, R.A., "Electrical Discharge Nitriding of High-strength Cast Iron," Metal Science and Heat Treatment, March pp. 159~162, 1964.

(3) Hudis, M., "Study of Ion-nitriding," Journal of Applied Physics, Vol. 44, No. 4, pp. 1489~1496, 1973.

(4) Jindal, P.C., "Ion nitriding of steels," Journal of Vacuum Science and Technology, Vol. 15, No. 2, pp. 313~317, 1978.

(5) Edenhofer, B. and Bewley, T.J., "Low-temperature Ion-nitriding: Nitriding at Temperatures below 500°C for Tools and Precision Machine Parts," Heat Treatment '76, Proceedings of the 16th International Heat Treatment Conference, The Metals Society, 1976.

(6) Cho, K.S. and Lee, C.O., "Wear Characteristics of Ion Nitrided Steel," Wear, Vol. 64, pp. 303~310, 1980.

(7) Jones, B.K. and Martin, J.W., "Residual Stress Distribution in Nitrided En 41B Steel as Function of Case Depth," Metals Technology, November pp. 520~523, 1977.

(8) Kwak, B.M. and Kim, J.D., "Determination of Mechanical Properties of Ion-nitrided Steel and Residual Stress Distribution," Transactions of the Korean Society of Mechanical Engineers, Vol. 5, No. 1, pp. 23~29, 1981.

(9) Ogurtani, T.O. and Uygur, E.M., "Diffusion of Nitrogen in Niobium, with Special Reference to Temperature Dependence of the Activation Energy," Transactions JIM., Vol. 13, pp. 396~399, 1972.

(10) Ogurtani, T.O., "The Kinetics of Diffusion of Hydrogen in Niobium," Metallurgical Transactions, Vol. 2, November pp. 3035~3038, 1971.

(11) da Silva, J.R.G. and McLellan, Rex B., "Diff-

usion of Carbon and Nitrogen in B.C.C. Iron," Materials Science and Engineering, Vol. 26, pp. 83~87, 1976.

(12) Boley, B.A. and Weiner, J.H., Theory of Thermal Stress, John Wiley & Sons, New York, pp. 243~328, 1960.

(13) Rie, K.-T. and Lampe, T., "Plasmanitrieren von Eisenwerkstoffen in Kohlenstoffhaltigen Gasgemischen," Zeitschrift für Metallkunde, Vol. 73, pp. 349~353, 1982.

(14) Goldstein, J.I. and Moren, A.E., "Diffusion Modeling of the Carburization Process," Metallurgical Transactions A, AIME, Vol. 9 A, November pp. 1515~1525, 1978.